
Article:
Aitken, Laura, Quinn, Steven D. orcid.org/0000-0003-3442-4103, Perez-Gonzalez, Cibran et al. (3 more authors) (2016) Morphology-Specific Inhibition of β-Amyloid Aggregates by 17β-Hydroxysteroid Dehydrogenase Type 10. Chembiochem. pp. 1029-1037. ISSN 1439-7633

https://doi.org/10.1002/cbic.201600081

A EUROPEAN JOURNAL OF CHEMICAL BIOLOGY

CHEMBIOCHEM

SYNTHETIC BIOLOGY & BIO-NANOTECHNOLOGY

Accepted Article

Title: Morphology-specific inhibition of β-amyloid aggregates by 17β-hydroxysteroid dehydrogenase type 10

Authors: Laura Aitken; Steven D Quinn; Cibran Perez-Gonzalez; Ifor D.W. Samuel; J Carlos Penedo; Frank J Gunn-Moore

To be cited as: ChemBioChem 10.1002/cbic.201600081

Link to VoR: http://dx.doi.org/10.1002/cbic.201600081

A Journal of

ChemPubSoc Europe

www.chembiochem.org

WILEY-VCH

Morphology-specific inhibition of β-amyloid aggregates by 17β-hydroxysteroid dehydrogenase type 10

Laura Aitken,[a]# Steven D. Quinn,[b,c]#¶ Cibran Perez-Gonzalez,[c,d] Ifor D. W. Samuel,[b] J. Carlos Penedo[c,d]* and Frank J. Gunn-Moore[a]*

[a]School of Biology, University of St. Andrews, Medical and Biological Sciences Building, North Haugh, St Andrews, Fife, United Kingdom. KY16 9TF.

[b]Organic Semiconductor Centre, SUPA, School of Physics and Astronomy, University of St Andrews, North Haugh, St Andrews, Fife, United Kingdom. KY16 9SS.

[c]SUPA, School of Physics and Astronomy, University of St Andrews, North Haugh, St Andrews, Fife, United Kingdom. KY16 9SS.

[d]Biomedical Sciences Research Complex, University of St. Andrews, Biomolecular Sciences Building, North Haugh, St Andrews, Fife, United Kingdom. KY16 9ST.

[¶]Current address: WestCHEM, School of Chemistry, Joseph Black Building, University of Glasgow, University Avenue, Glasgow, United Kingdom. G12 8QQ.

[#] Authors contributed equally.

[*] To whom correspondence should be addressed

Email: fjg1@st-andrews.ac.uk, jcp10@st-andrews.ac.uk

Abstract

A major hallmark of Alzheimer's disease (AD) is the formation of toxic aggregates composed of the β-amyloid peptide (Aβ). Given that Aβ peptides are known to co-localize within mitochondria and interact with 17β-HSD10, a mitochondrial protein expressed at high levels in AD brains, we have investigated the inhibitory potential of 17β-HSD10 against Aβ aggregation across a range of physiological conditions. The fluorescence self-quenching (FSQ) of Aβ(1-42), labelled with HiLyte Fluor 555, was used as a sensing strategy to evaluate the inhibitory effect of 17β-HSD10 under well-established conditions to grow distinct Aβ morphologies. Our results indicate that 17β-HSD10 preferentially inhibits the formation of globular and fibrillar-like structures but has no effect on the growth of amorphous plaque-like aggregates at endosomal pH 6. This work provides insights into the dependence of the Aβ-17β-HSD10 interaction with the morphology of Aβ aggregates and how this impacts enzymatic function.

Keywords: β-Amyloid peptide; 17β-hydroxysteroid dehydrogenase type 10; Alzheimer's disease; fluorescence self-quenching; neurochemistry

Abbreviations

17β-HSD10	=	17β-hydroxysteroid dehydrogenase type 10
ABAD	=	amyloid-binding alcohol dehydrogenase
AD	=	Alzheimer's disease
AFM	=	atomic force microscopy
AICD	=	amyloid precursor protein intracellular domain
APP	=	amyloid precursor protein
Aβ	=	amyloid-β peptide
BACE	=	β-secretase
BBB	=	blood–brain barrier
CD	=	circular dichroism
DLS	=	dynamic light scattering
DMSO	=	dimethyl sulfoxide
EM	=	electron microscopy
ER	=	endoplasmic reticulum
ETC	=	electron transport chain
FSQ	=	Fluorescence self-quenching
HFIP	=	1, 1, 1, 3, 3, 3- hexafluoro-2-propanol
Hsp	=	heat shock protein
MES	=	2-(N-morpholino)ethanesulfonic acid
ROS	=	reactive oxygen species
STD NMR	=	saturated transfer difference NMR
SDR	=	short chain dehydrogenase reductase
ThT	=	thioflavin T
TFE	=	tetrafluoroethylene
TIM	=	translocase of the inner membrane
TOM	=	translocase of the outer membrane

Introduction

Alzheimer's disease (AD) is the most common form of dementia, defined clinically as a progressive loss of declarative memory leading to complete social dependence and eventual death. It is characterized by cerebral extracellular amyloid plaques and intracellular neurofibrillary tangles.[1] The molecular mechanisms governing AD pathogenesis are still not fully understood [2,3] owing to its intrinsic complexity and no effective treatment has been developed to date. Nevertheless, it has been shown that the polymerization of the β-amyloid peptide (Aβ) into amyloid fibrils, and other morphologies including plaques and oligomeric species, constitutes a hallmark of AD.[4] The development of Aβ inhibitors has thus received much attention, with peptides[5–7] and small organic molecules[8–10] now established as the two main classes of amyloid inhibitors. Aβ production, aggregation and accumulation within the brain is summarised in **Figure 1**.

Since the discovery that Aβ peptides are found within the mitochondria of AD brains,[11] several attempts have been made to comprehend the mechanisms underpinning Aβ-induced mitochondrial dysfunction,[12–20] and to identify receptors which may be involved in this process.[21] Specifically, the observed interaction between mitochondrial proteins with aggregated Aβ peptides has been suggested as a potential pathogenic mechanism contributing to Aβ neurotoxicity in AD.[17-22] For instance, the 17β-hydroxysteroid dehydrogenase type 10 (17β-HSD10) or also commonly known as amyloid-binding alcohol dehydrogenase (ABAD))[21,23–26] constitutes one of such mitochondrial Aβ-interacting proteins.[6,27] 17β-HSD10 is a 27 kDa multifunctional enzyme expressed in all cell types and is thought to play a central role in the β-oxidation of fatty acids,[24,28] isoleucine degradation, catalysis and oxidation of alcohols and the reduction of aldehydes and ketones.[22] In transgenic mouse models for AD and in human AD sufferers, 17β-HSD10 has been shown to have increased expression levels and has gained considerable attention as a result of its ability to bind Aβ, suppress Aβ-induced apoptosis and free-radical generation in neurons.[11] It is known that the interaction between 17β-HSD10 and Aβ(1-40), Aβ(1-42) and Aβ(1-20) takes place in the nanomolar range (K_d ~ 40-80 nM),[11] which agrees well with the low cellular concentrations of Aβ peptide expected at the

early stages of AD. In addition, mutagenesis and inhibition studies have suggested that the L_D loop of 17β-HSD10, comprising residues C91-D119, plays a critical role in Aβ binding.[11] However, the lack of electron density for Aβ and the L_D loop of 17β-HSD10 in the crystal structure of the complex precluded the detailed characterization of the binding interface. A recent NMR study suggested that the 17β-HSD10/Aβ interaction takes place mostly via contacts between Aβ residues 17-20 (LVFF) and hydrophobic residues within the L_D loop.[29] Importantly, saturation transfer difference (STD-NMR) experiments also suggested that Aβ and nicotinamide adenine dinucleotide (NAD) binding to 17β-HSD10 are mutually exclusive, thus providing an explanation regarding how Aβ-binding may alter the activity of 17β-HSD10.[29] The interaction between 17β-HSD10 and Aβ *in vivo* has also been further demonstrated within mitochondria using co-localization and co-immunoprecipitation techniques,[11] but there are still many aspects of this interaction that remain poorly understood.

Here, we have employed a fluorescence self-quenching (FSQ) approach to investigate the interaction between 17β-HSD10 and amyloid aggregates. FSQ is based on the site-specific positioning of a fluorescent dye (HiLyte Fluor 555, **Figure S1**) at the N-terminal of the Aβ sequence. In FSQ, the fluorescence of the dye is maximal for non-aggregated Aβ but becomes progressively quenched as monomers aggregate, resulting in a combination of partially-quenched and non-emissive fluorophores (**Figure 2**) that decrease the overall fluorescence emission as aggregation progresses. The advantages of FSQ as an alternative to assays based on the binding of extrinsic dyes such as Thioflavin-T (ThT) to Aβ aggregates have been recently discussed.[29,33-35] There are many reasons for this work, firstly we want to determine the applicability of FSQ methods to investigate the interaction between amyloid and 17β-HSD10 as it has been previously shown for the interaction between Aβ and the 20 kDa heat shock protein (Hsp20).[33] Secondly, despite evidence for an in vivo association of 17β-HSD10 and Aβ sequences, it is not known whether 17β-HSD10 inhibits equally all amyloid morphologies or, in contrast, exhibits a certain degree of selectivity for some types of amyloid aggregates. In addition to inhibit amyloid aggregation, it has been shown that 17β-HSD10 in complex with Aβ becomes dysfunctional and its enzymatic inactivation leads to an increase in

mitochondrial stress and ultimately loss of neuron viability.[36] However, no *in vitro* data has been reported to confirm this aspect and it is unclear how both consequences of the interaction between 17β-HSD10 and Aβ, inhibition of aggregation and enzymatic inactivation of 17β-HSD10, relate to each other.

Our results using FSQ demonstrate that 17β-HSD10 specifically inhibits the formation of NaCl-induced fibrils and globular aggregates but has no effect on the formation of plaque-like structures grown at conditions mimicking endosomal pH. Furthermore, using an absorbance assay that monitors the conversion of NADH into NAD^+, we investigated the impact of these morphologies on the function of 17β-HSD10. It was found that although the formation of fibrils and globules is inhibited to similar levels by 17β-HSD10, their influence on 17β-HSD10 function is significantly different, with fibrillary structures showing the highest level of enzymatic inhibition. Lastly, a comparison between FSQ and the widely used ThT-based assay revealed that the ThT reporter dye exhibits, even in the absence of amyloid, a significant time-dependent fluorescence enhancement under the aggregation conditions used to promote the formation of globular amyloid structures. Thus, our findings highlight the limitations of ThT-based methods to monitor aggregation across different conditions and confirm that FSQ-based assays constitute a superior analytical tool to investigate amyloid self-assembly and when searching for small-molecule or protein-based inhibitors of this process.

Results

Monitoring amyloid aggregation and inhibition using fluorescence self-quenching

Aggregation of Aβ(1-42) functionalized at the N-terminal with HiLyte Fluor 555 ($Aβ_{555}$) into three different morphologies, namely globules, fibrils and plaques, was studied in real-time by fluorescence self-quenching (FSQ) at $Aβ_{555}$: 17β-HSD10 molar ratios of 1:0 (control), 1:1 and 2:1 as described in the Experimental Section. The rationale for choosing these morphologies was two-fold. Firstly, they constitute representative examples of the vast array of amyloid morphologies than can

be generated as a function of environmental conditions.[43] Secondly, aggregation protocols to reproducibly promote the formation of these Aβ(1-42) aggregates are well-established and the resulting aggregates have been extensively characterized using structural imaging methods including atomic-force microscopy (AFM) and electron-microscopy (EM).[32–51] In a previous study we have already shown using EM that the presence of the HiLyte Fluor 555 dye at the N-terminus of the Aβ(1-42) peptide ($A\beta_{555}$) does not affect the aggregation kinetics or the morphology of the aggregates.[34] Indeed, we observed amyloid structures of $A\beta_{555}$ with diameters of ~ 4 nm (fibrils) and ~ 22 nm (globules) which are identical to those obtained in the absence of N-terminal functionalization.[32,33,52] At pH 6 and pH 4 we observed the formation of amorphous plaque-like aggregates, as previously reported under similar acidic conditions.[52]

After having clarified the similar structural and kinetic behavior of $A\beta_{555}$ compared with unlabelled Aβ(1-42) and before describing our findings in the context of its application to the interaction between Aβ and 17β-HSD10, it is worth to briefly summarize the concept of FSQ-based assays. FSQ methods rely on the close positioning of the dyes induced by the tight packing of amyloid chains in the aggregated structure that triggers a very efficient quenching mechanism. This self-quenching mechanism is responsible for the observed time-dependent decrease in fluorescence emission of the HiLyte Fluor 555 dye[34] as the aggregation progresses and depends on the proximity and local density of identical dyes in the neighborhood of a given fluorophore **(Figure 2)**. An in-register parallel beta-sheet packing placing the N-terminal domains next to each other, has been recently reported using solid-state NMR,[43] thus providing a molecular-level explanation of how the organization of the amyloid fibrils enables a very efficient self-quenching process. As suggested in that work, hydrophobic assembly of two or more of these protofibrils might be possible and this could additionally contribute to place the dyes in close proximity.[43]

17β-HSD10 inhibits the formation of fibril-like structures

The kinetics of amyloid aggregation and the predominant morphologies arising from this process are known to be extremely sensitive to environmental conditions including pH, temperature and ionic strength.[42,52] For instance, we have previously demonstrated by TEM, FSQ and ThT assays that fibrillary structures constitute the predominant morphology at pH 7.9 and moderate concentrations of NaCl (150 mM).[33] Here, we used similar conditions to determine the impact of 17β-HSD10 on the formation of these amyloid aggregates. In the absence of 17β-HSD10 when a non-aggregated solution of 1 μM $A\beta_{555}$ was incubated in 50 mM Tris-HCl, 150 mM NaCl buffer (pH 7.9) at 37°C, we observed a decrease in the fluorescence intensity of 23.1 ± 1.2 % (**Figure 3A**). In the case where 1 μM $A\beta_{555}$ was induced to aggregate in the presence of 17β-HSD10 under the same experimental conditions, significant levels of inhibition were detected at the two $A\beta_{555}$: 17β-HSD10 molar ratios investigated. Specifically, the fluorescence intensity was quenched by 7.7 ± 0.5 % when the molar ratio was 2:1 (**Figure 3B**) and decreased to undetectable levels at an $A\beta_{555}$: 17β-HSD10 molar ratio of 1:1 (**Figure 3C**).

In order to validate and compare our FSQ assay against those already available, we used ThT as a sensor of amyloid fibril aggregation.[38] ThT (1.5 μM) acting on unlabelled Aβ(1-42) in 50 mM Tris, 150 mM NaCl (pH 7.9) buffer undergoes a 60.4 ± 0.7 % enhancement of fluorescence emission and exhibits a time-dependence for the aggregation process similar to that previously observed using FSQ, with both methods reaching a plateau at ~ 50 minutes (**Figure 3A**). At an $A\beta_{555}$: 17β-HSD10 molar ratio of 2:1, the ThT fluorescence enhancement decreased to a value of 8.1 ± 0.2 % (**Figure 3B**) and at 1:1 molar ratio no ThT enhancement was detected (**Figure 3C**). Thus, in agreement with the data obtained using FSQ, the ThT-based assay confirms that 17β-HSD10 interacts with Aβ(1-42) and efficiently inhibits the formation of amyloid fibrils in a concentration-dependent manner. The fluorescence spectra of $A\beta_{555}$ obtained at the different Aβ:17β-HSD10 molar ratios used are shown in **Figure S2** and the quenching rates obtained from the global fit of the aggregation profiles at 1:0 and 2:1 $A\beta_{555}$: 17β-HSD10 molar ratios using FSQ and ThT are summarized in **Table S1**.

A dependence of the inhibitory effect of 17β-HSD10 with the $A\beta_{555}$: 17β-HSD10 molar ratio agrees well with the observation that 0.5 μM concentrations of '*in vitro* aged' Aβ(1-42) had no effect on the dehydrogenase activity of the enzyme, whereas a 10-fold increase in Aβ(1-42) concentration caused substantial inhibition (~ 50 %) of 17β-HSD10 activity.[23] The inhibitory effect observed here for 17β-HSD10 against fibrillary aggregates is similar to that observed for other proteins with no reported chaperone activity such as β-lactoglobulin, α-lactalbumin and lysozyme.[58] These proteins have been shown to delay the formation of fibrillar aggregates at 1:1 molar ratios (protein: Aβ), whereas the enzyme catalase and pyruvate kinase completely suppressed amyloid aggregation at a much lower molar ratio of 1:100 (protein: Aβ).[58] Several mechanisms have been proposed to explain the inhibitory effect of these proteins at sub-stoichiometric amounts, including the interaction with monomeric peptides present in the β-sheet conformation and the formation of complexes with pre-fibrillar oligomers to slow down or prevent their growth into fibrils. It is unclear at this stage whether the inhibitory effect we observed for 17β-HSD10 towards the formation of fibrillar oligomers using both FSQ- and ThT-based assays shares similar mechanisms as those acting on non-chaperone proteins. However, the fact that no interaction between 17β-HSD10 and monomeric Aβ has been observed using SPR experiments,[11] and that no binding was observed in the NMR titration of 17β-HSD10 into amyloid monomers[29] suggests that 17β-HSD10 might act by forming dead-end Aβ: 17β-HSD10 aggregates as observed for β-lactoglobulin and catalase using ^{1}H-^{15}N-HSQC NMR spectroscopy.

17β-HSD10 inhibits the formation of rapidly growing globular aggregates

The formation of soluble amyloid oligomers and spherical aggregates is known to induce rapid cell degeneration, thus suggesting that soluble Aβ aggregates might have an increased toxicity over plaques and Aβ fibrils.[51] The formation of these globular species is known to be accelerated in the presence of lipids and other interfaces; a process that under certain conditions may lead to the formation of Aβ pores that disrupt the cellular membrane.[48] The addition of small amounts of

fluorinated solvents such as 1,1,1,3,3,3-hexafluoro-2-propanol (HFIP) and 2,2,2-tri-fluoroethanol (TFE) as co-solvents to a solution of monomeric Aβ has been demonstrated as a method to induce the formation of amyloid aggregates.[46] For instance, it has been shown that HFIP concentrations ≤ 4 % (v/v) induce the formation of globular structures *in vitro*.[42] HFIP droplets formed at these concentrations in an aqueous solution have been hypothesised to act as a growing interface where amyloid monomers can nucleate and accelerate growth as observed at the interface of biomimetic membranes including ganglioside micelles and lipid-rafts.[48] Moreover, it has been proposed that the toxicity of these globular structures may be responsible for the cognitive problems associated to the use of polyfluorinated anaesthetic compounds.[55]

To investigate the interaction and potential inhibitory properties of 17β-HSD10 under these globular forming conditions, we carried out FSQ experiments using 1.5 % (v/v) HFIP. We have previously shown that this concentration of HFIP induces Aβ aggregation over a time window of several minutes that can be easily followed in real-time using FSQ as the optical readout.[33-34] In the absence of 17β-HSD10, the addition of 1.5 % (v/v) HFIP to a non-aggregated solution of 1 μM $A\beta_{555}$ in 50 mM Tris-HCl buffer (pH 7.9) at 4°C under continuous agitation induced a decrease in fluorescence intensity of 60 ± 4 % over a 30-minute timescale (**Figure 4A**). When 1 μM $A\beta_{555}$ was induced to aggregate under the same experimental conditions, but in the presence of the 17β-HSD10 at $A\beta_{555}$: 17β-HSD10 molar ratios of 2:1 and 1:1, the self-quenching efficiencies were measured to be 19 ± 4 % and 13 ± 3 %, respectively (**Figure 4A**). Importantly, no quenching was observed in a similar 30-minute time window when $A\beta_{555}$ and 17β-HSD10 were incubated at a 1:1 molar ratio in the absence of HFIP (**Figure S3**), confirming that under these conditions, 17β-HSD10 interacts with Aβ during the HFIP-induced self-assembly process.

For comparative purposes, we have also explored the use of ThT fluorescent enhancement to monitor the formation of these globular structures and its inhibition by 17β-HSD10. Interestingly, we have found that the real-time injection of < 4% (v/v) HFIP to a buffered solution of 1.5 μM ThT (50 mM Tris-HCl buffer, pH 7.9, at 4°C) induces a significant increase (~ 4-fold) in its fluorescence

emission over a 5-10 minute time period, even in the absence of amyloid (**Figure 4B**). ThT emission enhancement has been extensively used as a reporter of HFIP-induced aggregation[41,45] and the emissive behaviour of the ThT dye in different restricted media including β-sheet and non-β-sheet cavities such as cyclodextrin, polymer films and micelles has been discussed in detail.[45] In contrast, no detailed investigation of ThT emission in mixtures of water and polyfluorinated solvents, which are known to form microdroplets and solvent clusters, has been reported.[47] However, the formation of HFIP micro-droplets acting as adsorption platforms for bovine serum albumin has already been discussed using TEM[42] and micro-heterogeneities in HFIP-water mixtures have been studied in detail using NMR and small angle neutron scattering (SANS) experiments revealing a correlation in lengths ranging from 7 to 10 Å.[54] Interesting these lengths match the diameter (8-9 Å) of γ-CD cavities which are known to promote the characteristic enhancement in ThT emission.[45] From NMR and SANS data it has been suggested that these micro-heterogeneities are maximized at HFIP concentrations of 30-35 % (v/v) and that the clusters organize with the trifluoromethyl (CF_3) groups pointing inside the core and hydroxyl (OH) groups forming hydrogen bonds with the surrounding water molecules.[54] At lower concentrations of HFIP (< 5 % v/v) oligomers have been detected by mass spectrometry but their size and stoichiometry remains unknown.[54]

The influence of HFIP on the photophysical properties of the ThT dye in aqueous solution was further investigated by monitoring its absorption spectrum as a function of HFIP concentration. We observed a significant decrease in the absorption values with the addition of 1.5 % (v/v) and 4 % (v/v) concentration of HFIP (**Figure S4**), whilst higher concentrations (~ 30 %) reversed this behaviour and additionally shifted the absorption maximum (**Figure S4**). Similar features were found for the absorption (**Figure S5A**) and emission spectra (**Figure S5B**) when replacing HFIP by TFE, although for the latter the effect required to induce a similar change is less pronounced. Our data suggest that the observed variation in the photophysical properties of ThT might arise from an interaction with the droplet-water interface that alters its molecular-rotor properties or from local changes in the dielectric constant that are known to influence ThT emission[47] and they clearly indicate that care

should be taken when interpreting its use as a reporter of amyloid aggregation in mixtures of water and polyfluorinated solvents.

In view of the uncertainties associated with the use of ThT to monitor HFIP-induced aggregation and taking into account the spherical organization of the globular aggregates, we decided to employ dynamic light scattering (DLS) as an alternative method to contrast our FSQ results and determine how these HFIP-induced aggregates are affected by the presence of 17β-HSD10. In the absence of 17β-HSD10, the values for the hydrodynamic radius (R_H) are broadly distributed between 60 nm and 400 nm (**Table S2**). These values are in good agreement with those previously reported by DLS and multi-angle light scattering (200-300 nm) for globule growth at similar HFIP concentrations.[41] Upon incubation with 17β-HSD10, a marked decrease in the R_H was observed at both Aβ:17β-HSD10 molar ratios of 2:1 and 1:1, where values of 44.9-108.0 nm and 36-150 nm were observed respectively (**Table S2**), corresponding to a decrease in molecular mass close to an order of magnitude. We interpret this decrease in average R_H as additional evidence for the inhibitory effect of 17β-HSD10 on globular aggregates.

Taken together, the FSQ and DLS data provide clear evidence for 17β-HSD10 inhibiting the formation of globular aggregates and suggests that the interaction of 17β-HSD10 with Aβ(1-42) must take place at a rate that competes with the relatively fast average aggregation rate reported for the globular aggregate (< 2 min^{-1}).[34] It has been shown previously that freshly prepared HFIP-induced globules are highly unstable against dilution and evolve over time into more stable and still soluble fibrillar aggregates.[34,42] Based on this, we hypothesize that a potential pathway to explain the inhibitory action of 17β-HSD10 towards globular species may involve the interaction and sequestering of Aβ material that is in dynamic exchange with the globular structures. The concept of an equilibrium between globules and low-molecular weight Aβ structures is strongly supported by the evolution of these globules into more stable structures over time. Remarkably, the ability of 17β-HSD10 to disrupt the formation of globular aggregates is significantly more pronounced than that reported for chaperone proteins including αB-crystallin[57] and the small heat shock protein 20

(Hsp20),[33] which constitute examples of the body's defense against protein misfolding.[33] For instance, wild-type Hsp20 does not show any ability to interfere with the formation of globular aggregates even at Aβ:Hsp20 molar ratios (1:2) higher than those employed here for 17β-HSD10.[33]

17β-HSD10 does not inhibit amorphous plaque-like aggregate formation in acidic conditions

It has been established that Aβ peptides are found within the mitochondria of AD brains[11] and it has been suggested that soluble Aβ aggregates (monomeric and oligomeric structures) enter the mitochondria via the transporter outer membrane (TOM) machinery.[12] As a mitochondrial protein, we hypothesised that 17β-HSD10 is unlikely to interact with large plaque-like material usually found to aggregate in lysosome environments under slightly acidic conditions (pH 6); however, to date, no direct experimental evidence had been reported to confirm this. Therefore, we decided to take advantage of the robustness of FSQ-based methods over a wide pH range to test the potential interaction between 17β-HSD10 and plaque-like aggregates formed at similar $A\beta_{555}$: 17β-HSD10 molar ratios as those used to investigate the interaction with globules and fibrils. In the control experiment, a solution of 1 μM $A\beta_{555}$ in 50 mM MES buffer (pH 6) at 37 °C induced a decrease in fluorescence intensity of 21.1 ± 0.5 % over a 50-minute timescale (**Figure 5A**). However, no significant inhibition was detected at $A\beta_{555}$: 17β-HSD10 molar ratios of 2:1 and 1:1. Under such conditions, the degree of FSQ remained largely invariant, with quenching values of 21.1 ± 0.9 % and 14.4 ± 0.7 %, respectively (**Figure 5B, C**). N-terminally labelled HiLyte Fluor 555 Aβ(□□42) quenching rates obtained under these conditions in the presence and absence of 17β-HSD10 are shown in **Table S3** and the fluorescence spectra obtained at the different molar ratios are shown in **Figure S6.**

Although amyloid staining methods based on extrinsic probes, such as ThT, are known to suffer from a decrease in affinity as high as 30-fold when the pH decreases from pH 8.5 to pH 6,[40] they have been previously used to monitor aggregation at endosomal pH. For comparison with the FSQ data, we carried out an identical set of experiments using the emission of ThT as a probe. For unlabelled Aβ (1-42) in the absence of 17β-HSD10 we observed a 32.0 ± 0.2 % enhancement of

fluorescence over a 50-minute time scale (**Figure 5A**). At Aβ (1-42): 17β-HSD10 molar ratios of 1:1 and 2:1, the overall ThT enhancement remained largely invariant and emission enhancements of 23.6 ± 0.3 % and 22.8 ± 0.2 % were observed, respectively (**Figure 5B, C**). The observation using ThT that 17β-HSD10 does not inhibit aggregation at pH 6 is therefore entirely consistent with our analysis using FSQ.

Amyloid-induced inactivation of 17β-HSD10 enzymatic function

17β-HSD10 is the only human protein found to interact with Aβ in a yeast two-hybrid screening,[21] suggesting that Aβ-induced cytotoxicity takes place mostly through its interaction with 17β-HSD10.[18,36,50] The current hypothesis suggests that HSD10 in complex with Aβ becomes dysfunctional and leads to an increased mitochondrial stress and ultimately loss of neuron viability.[50] The inhibitory effect of Aβ(1-42) on 17β-HSD10 binding to the NADH/NAD^+ cofactor has already been confirmed using surface-plasmon resonance (SPR) and saturation transfer difference (STD) NMR experiments.[29] However, the precise morphological state of Aβ(1-42) that inactivates 17β-HDS10 has not been established. Our FSQ data indicates that 17β-HDS10 interacts with fibrillar and globular amyloid structures but not with plaques; therefore, we decided to investigate the enzymatic activity of 17β-HDS10 under fibril- and globule-growing conditions.

Before assessing the influence of amyloid aggregation state on the function of 17β-HSD10, it was important to ascertain if the enzyme itself was active in the specific buffers required to promote these morphologies. For this, we employed an assay that monitors changes in NADH absorbance. During the conversion of substrate (acetoacetyl coenzymeA) to product, 17β-HSD10 uses NADH as a cofactor, converting it to NAD^+. Thus, the loss of absorbance of NADH at 340 nm (as it is converted to NAD^+) is a measure of 17β-HSD10 activity (**Figure 6A**). Specific activity values for 17β-HSD10 were calculated in μmol min^{-1} mg^{-1} for this assay, and the background observed in the negative control (when no 17β-HSD10 is present in the reaction mixture) is minimal with values of around 0.2 μmol min^{-1} mg^{-1}, compared to positive control values of approximately 4 μmol min^{-1} mg^{-1} for a reaction

mixture containing 5 μg/ml 17β-HSD10 (**Figure 6B**). Under both oligomeric/ fibril like (50 mM Tris-HCl buffer solution containing 150 mM NaCl) and globular aggregation buffer conditions (50 mM Tris-HCl (no NaCl), 1.5 % (v/v) HFIP) there was no change in specific 17β-HSD10 activity (**Figure 6B**). Under plaque-growing conditions (pH 6.0, 50 mM MES, 37°C) only a very slight decrease in 17β-HSD10 activity (< 4 %) was observed (**Figure 6B**).

When the absorbance assay was repeated at conditions that induce the real-time aggregation of amyloid we observed a morphology-dependent response. At fibril-growing conditions, the level of enzymatic inhibition showed a dependence with the Aβ(1-42):17β-HSD10 molar ratio. At 1:1 and 2:1 molar ratios, the enzymatic activity decreased by 3.4 ± 1.9 % and 20.2 ± 1.6 %, respectively (**Figure 6C**). When we used experimental conditions that promote the formation of globular structures, we observed a very moderate decrease in the enzymatic activity (5.4 ± 1.7 %), even at the highest 5:1 Aβ(1-42):17β-HSD10 molar ratio employed. Taken together, these data suggest that certain amyloid morphologies exhibit higher toxicity levels towards 17β-HSD10 function and confirm that, in a rich amyloid environment, the formation of Aβ(1-42) fibrils has a deleterious effect on 17β-HSD10 activity.

Discussion

A bar plot summarizing the relative variation in fluorescence self-quenching observed for the aggregation of 1 μM $A\beta_{555}$ into globular, fibrils and amorphous plaque-like aggregates in the presence and absence of 17β-HSD10 is shown in **Figure 7A** and compared with the results from a ThT-based assay for fibrils and plaques in **Figure 7B**. Overall, both methods provided strong evidence for 17β-HSD10 preferentially interacting with certain amyloid morphologies. Specifically, 17β-HSD10 demonstrated inhibitory potential towards globular and fibrillar structures formed at neutral conditions, but it displayed no effect on the aggregation mechanism of plaque structures formed *in vitro* at pH 6. A certain degree of preferential interaction of 17β-HSD10 with some amyloid aggregates could be anticipated based on the crystal structure of the 17β-HSD10/ Aβ(1-42) complex

that reveals the presence of a large cavity (~ 70 Å) that could easily accommodate fibrillar structures (40-60 Å), but not, for instance, plaque-like aggregates.[11]

The stoichiometry of the Aβ-17β-HSD10 complex has not yet been determined but it has been hypothesized that 17β-HSD10 does not interact with Aβ(1-42) monomers during surface plasmon resonance (SPR) and nuclear magnetic resonance (NMR) experiments.[11,29] Therefore, it is unlikely that physical and/or structural differences between the monomeric state of Aβ(1-42) at different pH can account for the observed discrimination between plaque-like structures formed at pH 6 and fibrils and globules formed at neutral conditions. Moreover, 17β-HSD10 at identical conditions as those used to generate amorphous plaque-like aggregates showed enzymatic levels comparable to neutral pH (**Figure 6B**), confirming that the numerous interactions the substrate forms with loops L_F, L_E and L_D are conserved at slightly acidic conditions. In particular, the L_D loop region which has been shown by mutagenesis studies and NMR analysis to be the 17β-HSD10 interface with Aβ,[29] should remain accessible for Aβ binding.

Since in all our *in vitro* assays, 17β-HSD10 is present in the aggregation mixture from the very early stages, we hypothesize that either differences in the structure of the aggregation intermediates or in the kinetics of the aggregation pathway between neutral and slightly acidic conditions may be responsible for the observed differences. This hypothesis is supported by experimental evidence suggesting that indeed both amyloid morphology and aggregation kinetics at pH 6, are remarkably different from those at neutral conditions.[39,60] Recent *in vivo* studies have also determined that intra-neuronal Aβ(1-42) aggregates faster in lysosomes and without a detectable lag phase, and this finding was justified in terms of the acidic environment bringing the peptide closer to its isoelectric point.[61] Using a combination of fluorescence methods and structural techniques, it has been shown that amyloid aggregation at pH 5.8 is characterized by the rapid formation (~ 10 seconds) of amorphous aggregates with sizes ranging from 50 to 500 nm.[40] Importantly, as determined by circular dichroism (CD), these aggregates do not contain α-helical or β-structure and they are unable to seed fibril formation.[40] It has also been demonstrated that the aggregates evolve into smaller

structures (30-80 nm) after 30 minutes which agrees well with the time window of the aggregation process observed in our FSQ and ThT experiments (**Figure 5**). The time scale of the initial growth phase is within our mixing time, so it is likely that with the time resolution of our assay, we are monitoring the disappearance of the initially formed aggregates as they slowly evolve into other morphologies. As reported by Gorman and coworkers,[39] these slow-forming morphologies also displayed very little, if any, β-structure. However, a lack of β-sheet structure at acidic pH cannot exclusively account for the observed lack of aggregation inhibition, as it has been shown that 17β-HSD10 does not bind Aβ(25-35), which is known to exhibit a β-sheet conformation by CD and NMR studies.[63]

In contrast, the conformation of the N-terminal region, residues 17-20 of Aβ(1-20) that constitute the binding interface with 17β-HSD10,[11] is known to exhibit a random-coil/α-helix/β-sheet equilibrium that is highly dependent on pH conditions.[61,63,64] At pH 7-8, it has been demonstrated that residues 10-28, containing the putative 17β-HSD10 binding interface, are in equilibrium between random coil and α-helix conformations. In the region between pH 4-7, this equilibrium includes a further β-sheet conformation. Taken together, our data suggests that such pH-induced conformational re-arrangements of the N-terminal may be crucial to modulating the specific interaction of 17β-HSD10 with certain amyloid morphologies.

We further extended our analysis of the interaction between Aβ(1-42) and 17β-HSD10 to explore how the different aggregation conditions impact the enzymatic activity. Our results indicate that although 17β-HSD10 can efficiently inhibit the formation of fibrils and globules, rich amyloid conditions that promote the formation of fibrillar structures constitute the more toxic environment inducing a 20.2 % decrease in enzymatic function (**Figure 6C**). As previously discussed, the crystal structure of 17β-HSD10 bound to Aβ indicates the presence of a large solvent cavity involving the L_D loop with estimated dimensions of 70 Å. These dimensions are relatively close to the diameter of amyloid fibrils (4-6 nm) but much smaller than the average diameter (~ 22 nm) measured by TEM and DLS for globular structures.[34,42] Therefore, it is possible that the higher enzymatic inhibition

observed under fibril-forming conditions is arising from the ability of these structures to drift and fit into this cavity and block the active site region, thus inactivating the enzyme.

Our data also provides evidence for an uncoupling between the determinants that influence the formation of Aβ/17β-HSD10 complexes and those that mediate suppression of enzymatic activity by amyloid fibrils at much higher Aβ concentrations. The observation that high Aβ(1-42): 17β-HSD10 molar ratios of amyloid are required to have a significant impact on activity agrees well previous studies where the concentration of Aβ required for half-maximal inhibition was in the micromolar range (1-3 μM) rather than the nanomolar range (~ 40 nM) required for efficient binding and most likely present at intracellular level.[18] The need for a rich amyloid environment to impair activity is also further supported by *in vivo* studies using SH-SY5Y human neuroblastoma cells that showed a decrease in the efficiency of 17β-HSD10 catalyzed estradiol to estrone conversion upon incubation with a high concentration of Aβ.[50] It has been suggested that the N-terminal domain of Aβ may be involved in the initial association to 17β-HSD10, and in a rich amyloid environment, the C-terminal portion is free to interact and recruit additional Aβ molecules resulting in a macromolecular complex that distorts the enzyme and alters its function.[18] Evaluating all this evidence together, we hypothesize that intracellular amyloid toxicity is not exclusively arising from the formation of Aβ/17β-HSD10 complexes but it is amplified by this secondary recruitment of amyloid molecules that may disrupt (for example) the quaternary organization of the enzyme, modify its substrate specificity or its localization and thus increase cell vulnerability.

Conclusion

The biophysical characterization of the Aβ/17β-HSD10 interaction is pivotal for a full understanding of the interaction between Aβ accumulated inside nerve cells and intracellular proteins. Unfortunately, the exact details of the Aβ/17β-HSD10 interaction have remained elusive by X-ray crystallography and, as demonstrated here, ThT-based methods to monitor amyloid aggregation and its inhibition by 17β-HSD10 are not suitable at all experimental conditions. Consequently, the range

of amyloid morphologies capable of interacting with 17β-HSD10 has remained elusive. In the present study, we took advantage of the robustness of fluorescence self-quenching methods to monitor the inhibitory efficiency of 17β-HSD10 against a range of amyloid morphologies. Our results demonstrate preferential inhibition towards globular and fibril-like aggregates formed under neutral conditions by 17β-HSD10. The lack of inhibition towards amorphous plaque-like aggregates, generated at slightly acidic conditions, was discussed in terms of the known influence of pH on the conformational equilibrium of the N-terminal fragment of the Aβ peptide, which contains the putative Aβ/17β-HSD10 binding interface. From the range of morphologies that were found to interact with 17β-HSD10, inhibition of acetoacetyl-CoA reduction was only detected at fibril-forming conditions and when Aβ(1-42) was present at concentrations much higher than those required for efficient binding. This work provides insights into the dependence of the Aβ/17β-HSD10 interaction with the morphology of amyloid aggregates and suggests that the determinants that mediate Aβ(1-42) binding to 17β-HSD10 are different from those than influence the suppression of 17β-HSD10 activity.

Experimental

All aqueous solutions were prepared with deionized water (Millipore, UK) and all chemicals purchased from Sigma Aldrich, UK unless stated otherwise.

17β-HSD10 Purification

Cell pellets of *E. coli* BL21-CodonPlus cells containing Histev-17β-HSD10 protein were re-suspended for 30 min, 4 °C, in lysis buffer (20 mM NaH_2PO_4, 30 mM imidazole, 500 mM NaCl, 10 % (v/v) glycerol, pH 7.5) with the addition of complete EDTA-free protease inhibitor tablets (Roche), lysozyme (1 mg/mL), DNase (20 μg/mL) and Triton X-100 (0.1 % (v/v)). Cells were lysed by passage through a cell disruptor at 30 kPSI (Constant Systems Ltd) and the lysate was cleared by centrifugation (Sorvall Evolution RC, rotor S5-34 55-34 angle, 20500 rpm, 30 min, 4 °C). Cleared

lysate was filtered (0.44 μm membrane; Whatman) then applied to a Ni-NTA (GE Healthcare) column pre-washed with lysis buffer and protein eluted with 300 mM imidazole buffer (20 mM NaH_2PO_4, 300 mM imidazole, 500 mM NaCl, 10 % (v/v) glycerol, pH 7.5). Tobacco etch virus (TEV) protease was added to the protein at a mass-to-mass ratio of 1:10, to cleave the histidine tag and the protein was then dialysed into 20 mM Tris-HCl, 30 mM imidazole, 500 mM NaCl, 10% (v/v) glycerol, pH 7.5 containing EDTA (1 mM) and DTT (1 mM) to aid solubility. Protein digestion and dialysis was carried out at 4 °C for 16 h.

Complete digestion was firstly checked by SDS- PAGE, then fully digested protein was passed over a second Ni-column and the flow-through, containing 17β-HSD10 protein, was concentrated using a Vivaspin column (10 kDa MWCO, GE Healthcare) to ~ 7 mL before final purification using gel filtration to remove imidazole (Hi-Load 16/60 Superdex 75 prep grade column, GE Healthcare, flow rate 1.5 mL/min). Protein was eluted in gel filtration buffer (10 mM Tris-HCl, 150 mM NaCl, 10% glycerol, pH 7.5) and concentrated (Vivaspin column (10 kDa MWCO, GE Healthcare)) to 10 mg/mL. Aliquots (10 μL) were taken and flash frozen in liquid nitrogen before final storage at -80 °C.

17β-HSD10 Activity Assay

17β-HSD10 was diluted from frozen stock solution to a 0.2 mg/mL working stock in assay buffer 10 mM Tris-HCl, 150 mM NaCl, 10 % (v/v) glycerol, pH 7.5 (at 30 °C). Acetoacetyl-CoA substrate (AcAcCoA) was prepared as a 4.8 mM stock in assay buffer, and nicotinamide adenine dinucleotide (NADH) was prepared as a 10 mM stock in assay buffer. Using a Nunc 96 well plate the enzyme activity assay was set up to give final assay concentrations as follows: 120 μM AcAcCoA, 250 μM NADH and 8 μg/mL 17β-HSD10. In order to initiate the reaction 17β-HSD10 is added and the initial rate is recorded over the first 30 s using the FLUOstar plate reader (BMG Labtech; parameters λ= 340 nM, T= 30 °C, 0.5 s orbital measuring intervals). Enzyme activity was calculated using, ε= 6220 M^{-1} cm^{-1} for NADH, where the NADH rate of consumption = AcAcCoA rate of reduction. Assays were performed by triplicate and the error was reported as ± SEM (standard error mean).

HiLyte Fluor 555

Synthetic dye labelled Aβ1–42 peptides incorporating HiLyte Fluor 555 were purchased from Anaspec Inc. (USA) and used with no additional purification, further details can be found in the supplementary information.

Amyloid Monomer Preparation and Fluorescence Spectroscopy of Aβ(1-42) Aggregates

The methods for amyloid monomer preparation and fluorescence spectroscopy of Aβ(1-42) aggregates can be found in the supplementary materials.

Aggregation protocols

Aggregation protocols for the three conditions investigated have been previously published [33,34,52] and details can be found in the supplementary materials.

Dynamic Light Scattering

Dynamic light scattering methods can be found in the supplementary materials.

Acknowledgements

This research is part-funded by the MSD Scottish Life Sciences fund. As part of an on-going contribution to Scottish life sciences, MSD Limited, a global healthcare leader, has given substantial monetary funding to the Scottish Funding Council (SFC) for distribution via the Scottish Universities Life Science Alliance (SULSA) to develop and deliver a high quality drug discovery research and training programme. All aspects of the programme have been geared towards attaining the highest value in terms of scientific discovery, training and impact. The opinions expressed in this research are those of the authors and do not necessarily represent those of MSD Limited, nor its Affiliates. This research was also kindly supported by Alzheimer's Society, specifically The Barcopel Foundation, EPSRC, and BBSRC.

Conflict of Interest

The authors declare no competing financial interest.

References

[1] K. S. Kosik, *Science*. **1992**, *256*, 780–783.
[2] M. P. Mattson, *Nature*. **2004**, *430*, 631–639.
[3] P. J. Crouch, S-M. E. Harding, A. R. White, J. Camakaris, A. I. Bush, C. L. Masters, *Int. J. Biochem. Cell Biol.* **2008**, *40*, 181–198.
[4] G. Yamin, K. Ono, M. Inayathullah, D. B. Teplow, *Curr. Pharm. Des.* **2008**, *14*, 3231–3246.
[5] C. Soto, E. M. Sigurdsson, L. Morelli, R. A. Kumar, E. M. Castaño, B. Frangione, *Nat. Med.*, **1998**, *4*, 822–826.
[6] T. Takahashi, H. Mihara, *Acc. Chem. Res.* **2008**, *41*, 1309–1318.
[7] A. Frydman-Marom, M. Rechter, I. Shefler, Y. Bram, D. E. Shalev, E. Gazit, *Angew. Chem. Int. Ed Engl.* **2009**, *48*, 1981–1986.
[8] F. Yang, G. P. Lim, A. N. Begum, O. J. Ubeda, M. R. Simmons, S. S. Ambegaokar, P. P. Chen, R. Kayed, C. G. Glabe, S. A. Frautschy, G. M. Cole, *J. Biol. Chem.* **2005**, *280*, 5892–5901.
[9] D. E. Ehrnhoefer, J. Bieschke, A. Boeddrich, M. Herbst, L. Masino, R. Lurz, S. Engemann, A. Pastore, E. E. Wanker, *Nat. Struct. Mol. Biol.* **2008**, *15*, 558–566.
[10] J. Geng, M. Li, J. Ren, E. Wang, X. Qu, *Angew. Chem. Int. Ed Engl.* **2011**, *50*, 4184–4188.
[11] J. W. Lustbader, M. Cirilli, C. Lin, H. W. Xu, K. Takuma, N. Wang, C. Caspersen, X. Chen, S. Pollak, M. Chaney, F. Trinchese, S. Liu, F. Gunn-Moore, L.-F. Lue, D. G. Walker, P. Kuppusamy, Z. L. Zewier, O. Arancio, D. Stern, S. S. Yan, H. Wu, *Science*. **2004**, *304*, 448–452.
[12] C. A. Hansson Petersen, N. Alikhani, H. Behbahani, B. Wiehager, P. F. Pavlov, I. Alafuzoff, V. Leinonen, A. Ito, B. Winblad, E. Glaser, M. Ankarcrona, *Proc. Natl. Acad. Sci.* **2008**, *105*, 13145 – 13150.
[13] N. Dragicevic, M. Mamcarz, Y. Zhu, R. Buzzeo, J. Tan, G. W. Arendash, P. C. Bradshaw, *J. Alzheimers Dis.* **2010**, *20*, S535–S550.
[14] H. Du, L. Guo, F. Fang, D. Chen, A. A. Sosunov, G. M. McKhann, Y. Yan, C. Wang, H. Zhang, J. D. Molkentin, F. J. Gunn-Moore, J. P. Vonsattel, O. Arancio, J. X. Chen, S. D. Yan, *Nat. Med.* **2008**, *14*, 1097–1105.
[15] H. Du, L. Guo, W. Zhang, M. Rydzewska, S. Yan, *Neurobiol. Aging*. **2011**, *32*, 398–406.
[16] H. Atamna, W. H. Frey 2nd, *Mitochondrion*. **2007**, *7*, 297–310.
[17] E. Borger, L. Aitken, K. E. A. Muirhead, Z. E. Allen, J. A. Ainge, S. J. Conway, F. J. Gunn-Moore, *Biochem. Soc. Trans.* **2011**, *39*, 868–873.
[18] S. D. Yan, D. M. Stern, *Int. J. Exp. Pathol.* **2005**, *86*, 161–171.
[19] W. D. Parker Jr, C. M. Filley, J. K. Parks, *Neurology*. **1990**, *40*, 1302–1303.
[20] E. M. Mutisya, A. C. Bowling, M. F. Beal, *J. Neurochem.* **1994**, *63*, 2179–2184.
[21] S. Du Yan, J. Fu, C. Soto, X. Chen, H. Zhu, F. Al-Mohanna, K. Collison, A. Zhu, E. Stern, T. Saido, M. Tohyama, S. Ogawa, A. Roher, D. Stern, *Nature*. **1997**, *389*, 689–695.
[22] K. E. A. Muirhead, E. Borger, L. Aitken, S. J. Conway, F. J. Gunn-Moore, *Biochem. J.* **2010**, *426*, 255–270.
[23] S. Du Yan, Y. Shi, A. Zhu, J. Fu, H. Zhu, Y. Zhu, L. Gibson, E. Stern, K. Collison, F. Al-Mohanna, S. Ogawa, A. Roher, S. G. Clarke, D. M. Stern, *J. Biol. Chem.* **1999**, *274*, 2145 –2156.
[24] A. Powell, J. Read, M. Banfield, F. J. Gunn-Moore, S. Du. Yan, J. Lustbader, A. Stern, D. Stern, R. Brady, *J. Mol. Biol.* **2000**, *303*, 311–327.
[25] S. Du Yan, Y. Zhu, E. D. Stern, Y. C. Hwang, O. Hori, S. Ogawa, M. P. Frosch, E. S. Connolly, R. McTaggert, D. J. Pinsky, S. Clarke, D. M. Stern, R. Ramasamy, *J. Biol. Chem.* **2000**, *275*, 27100 – 27109.
[26] J. Yao, H. Du, S. Yan, F. Fang, C. Wang, L.-F. Lue, L. Guo, D. Chen, D. M. Stern, F. J. Gunn-Moore, J. Xi Chen, O. Arancio, S. S. Yan, *J. Neurosci.* **2011**, *31*, 2313 –2320.
[27] E. Borger, L. Aitken, H. Du, W. Zhang, F. J. Gunn-Moore, S. Yan, *Curr. Alzheimer Res.* **2012**, *10*, 9-21.
[28] X. He, G. Merz, Y. Yang, P. Mehta, H. Schulz, S. Yang, *Eur. J. Biochem.* **2001**, *268*, 4899–4907.

[29] Y. Yan, Y. Liu, M. Sorci, G. Belfort, J. W. Lustbader, S. S. Yan, C. Wang, *Biochemistry* **2007**, *46*, 1724–1731.
[30] F. Meng, P. Marek, K. J. Potter, C. B. Verchere, D. P. Raleigh, *Biochemistry* **2008**, *47*, 6016–6024.
[31] S. A. Hudson, H. Ecroyd, T. W. Kee, J. A. Carver, *FEBS J.* **2009**, *276*, 5960–5972.
[32] W. B. Stine, K. N. Dahlgren, G. A. Krafft, M. J. LaDu, *J. Biol. Chem.* **2003**, *278*, 11612–11622.
[33] R. T. Cameron, S. D. Quinn, L. S. Cairns, R. MacLeod, I. D. W. Samuel, B. O. Smith, J. Carlos Penedo, G. S. Baillie, *Mol. Cell. Neurosci.* **2014**, *61*, 46-55.
[34] S. D. Quinn, P. A. Dalgarno, R. T. Cameron, G. J. Hedley, C. Hacker, J. M. Lucocq, G. S. Baillie, I. D. W. Samuel, J. C. Penedo, *Mol. Biosyst.* **2014**, *10*, 34–44.
[35] S. Freire, F. Rodríguez-Prieto, M. C. Ríos Rodríguez, J. C. Penedo, W. Al-Soufi, M. Novo, M. *Chem. – Eur. J.* **2015**, *21*, 3425–3434.
[36] K. Takuma, J. Yao, J. Huang, H. Xu, X. Chen, J. Luddy, A. C. Trillat, D. M. Stern, O. Arancio, S. S. Yan, *FASEB J* **2005**, *19*, 597-598.
[37] X. Zhuang, T. Ha, H. D. Kim, T. Centner, S. Labeit, S. Chu, *Proc. Natl. Acad. Sci.* **2000**, *97*, 14241–14244.
[38] W. L. Klein, *Neurochem. Int.* **2002**, *41*, 345–352.
[39] P. M. Gorman, C. M. Yip, P. E. Fraser, A. Chakrabartty, *J. Mol. Biol.* **2003**, *325*, 743–757.
[40] M. Lindgren, K. Sörgjerd, P. Hammarström, *Biophys. J.* **2005**, *88*, 4200–4212.
[41] T. Ban, D. Hamada, K. Hasegawa, H. Naiki, Y. Goto, *J. Biol. Chem.* **2003**, *278*, 16462-16465.
[42] M. R. Nichols, M. A. Moss, D. K. Reed, S. Cratic-McDaniel, J. H. Hoh, T. L. Rosenberry, *J. Biol. Chem.* **2005**, *280*, 2471–2480.
[43] Y. Xiao, B. Ma, D. McElheny, S. Parthasarathy, F. Long, M. Hoshi, R. Nussinov, Y. Ishii, *Nat. Struct. Mol. Biol.* **2015**, *22*, 499–505.
[44] N. Amdursky, Y. Erez, D. Huppert, *Acc. Chem. Res.* **2012**, *45*, 1548–1557.
[45] M. Groenning, L. Olsen, M. van de Weert, J. M. Flink, S. Frokjaer, F. S. Jørgensen, *J. Struct. Biol.* **2007**, *158*, 358–369.
[46] S. K. Pachahara, H. Adicherla, R. Nagaraj, *PLoS ONE*. **2015**, *10*, e0136567.
[47] A. A. Maskevich, V. I. Stsiapura, V. A. Kuzmitsky, I. M. Kuznetsova, O. I. Povarova, V. N. Uversky, K. K. J. Turoverov, *Proteome Res.* **2007**, *6*, 1392–1401.
[48] E. Y. Chi, S. L. Frey, A. Winans, K. L. H. Lam, K. Kjaer, J. Majewski, K. Y. C. Lee, *Biophys. J.* **2010**, *98*, 2299–2308.
[49] P. I. Moreira, K. Honda, Q. Liu, M. S. Santos, C. R. Oliveira, G. Aliev, A. Nunomura, X. Zhu, M. A. Smith, G. Perry, *Curr. Alzheimer Res.* **2005**, *2*, 403–408.
[50] Y. A. Lim, A. Grimm, M. Giese, A. G. Mensah-Nyagan, J. E. Villafranca, L. M. Ittner, A. Eckert, J. Götz, *PLoS ONE*. **2011**, *6*, e28887.
[51] A. Jan, D. M. Hartley, H. A. Lashuel, *Nat. Protoc.* **2010**, *5*, 1186–1209.
[52] W. B. Stine, L. Jungbauer, C. Yu, M. J. LaDu, *Methods Mol. Biol.* **2011**, *670*, 13–32.
[53] S. A. Kotler, P. Walsh, J. R. Brender, A. Ramamoorthy, *Chem. Soc. Rev.* **2014**, *43*, 6692–6700.
[54] K. Yoshida, T. Yamaguchi, T. Adachi, T. Otomo, D. Matsuo, T. Takamuku, N. Nishi, *J. Chem. Phys.* **2003**, *119*, 6132–6142.
[55] R. G Eckenhoff, J. S Johansson, H. Wei, A. Carnini, B. Kang, W. Wei, R. Pidikiti, J. M. Keller, M. F Eckenhoff, *Anesthesiology*. **2004**, *101*, 703–709.
[56] E. Vilardo, W. Rossmanith, *PloS ONE*. **2013**, *8*, e65609.
[57] P. Santhoshkumar, K. K. Sharma, *Mol. Cell. Biochem.* **2004**, *267*, 147–155.
[58] J. Luo, S. K. T. S. Wärmländer, A. Gräslund, J. P. Abrahams, *J. Biol. Chem.* **2014**, *289*, 27766–27775.
[59] X. Wang, Y. Yang, M. Jia, C. Ma, M. Wang, L. Che, Y. Yang, J. Wu, *Neural Regen. Res.* **2013**, *8*, 39–48.
[60] E. K. Esbjörner, F. Chan, E. Rees, M. Erdelyi, L. M. Luheshi, C. W. Bertoncini, C. F. Kaminski, C. M. Dobson, G. S. Kaminski Schierle, *Chem. Biol.* **2014**, *21*, 732–742.
[61] S. J. Wood, B. Maleeff, T. Hart, R. Wetzel, *J. Mol. Biol.* **1996**, *256*, 870–877.

[62] X. Chen, S. D. Yan, *IUBMB Life*. **2006**, *58*, 686–694.
[63] C. Soto, E. M. Castaño, B. Frangione, N. C. Inestrosa, *J. Biol. Chem.* **1995**, *270*, 3063–3067.
[64] K. Ma, E. L. Clancy, Y. Zhang, D. G. Ray, K. Wollenberg, M. G. Zagorski, *J Am Chem Soc*. **1999**, *121*, 8698–8706.

Figure Legends

Figure 1. Production, aggregation and accumulation of Aβ peptides within the brain is associated with neural dysfunction. Aβ peptides are formed within the cell membrane via cleavage of the amyloid precursor protein (APP) by β-secretase cleaving enzymes (BACEs). Soluble Aβ oligomers interact with cell-surface membranes and receptors, as well as intracellular components to lead to neuronal dysfunction. In particular, Aβ interactions with 17β-HSD10 in the mitochondria can lead to the inhibition of 17β-HSD10 activity which in turn leads to toxicity and mitochondrial dysfunction. Aβ can also self-assemble into pathogenic fibrils, plaques and other higher-order structures, displacing vital cellular components and leading to their malfunction.

Figure 2. Principle of the fluorescence self-quenching (FSQ) assay to monitor the aggregation of the β-amyloid (Aβ) peptide. **A)** HiLyte Fluor 555 fluorescence is progressively quenched via FSQ as monomers aggregate. This may lead to the combination of partially quenched and completely quenched (non-emissive) states. The morphology shown is for illustrative purposes only and the schematic is not drawn to scale. **B)** Variation in the emission spectra of HiLyte Fluor 555 attached to the N-terminal of Aβ(1-42) as a function of aggregation time and **C)** representative fluorescence intensity profile during aggregation of 1 μM $A\beta_{555}$ over a 30-minute time window. λ_{exc} = 547 nm.

Figure 3. Representative aggregation time courses obtained for 1 μM $A\beta_{555}$ using FSQ (black circles) and for unlabelled Aβ(1-42) using ThT enhancement (grey squares) under fibril forming conditions in the presence of 17β-HSD10 at Aβ:17-β-HSD10 molar ratios of **A)** 1:0, **B)** 2:1 and **C)** 1:1. Solid lines represent the results from a fit to a monoexponential decay function using non-linear squares fitting. Solid lines in **C)** represent the fitting to a straight line.

Figure 4. A) Representative aggregation time courses obtained using FSQ for the HFIP-induced aggregation of $A\beta_{555}$ in the presence of 17β-HSD10 at $A\beta_{555}$:17β-HSD10 molar ratios of 1:0 (black, control), 2:1 (blue) and 1:1 (red) as a function of time at 4 ^{o}C after injection of 1.5 % (v/v) HFIP. The solid lines are fits to exponential decay functions. **B)** ThT fluorescence enhancement in the absence of Aβ(1-42) at the indicated concentrations of HFIP.

Figure 5. Representative aggregation time courses obtained for 1 μM $A\beta_{555}$ using FSQ (black circles) and for unlabelled Aβ(1-42) using ThT enhancement (grey squares) at pH 6 in the presence of 17β-HSD10 at Aβ:17β-HSD10 molar ratios of **A)** 1:0, **B)** 2:1 and **C)** 1:1. Solid lines represent the results from a fit to a monoexponential decay function using non-linear squares fitting.

Figure 6. Absorbance screening assay used to assess 17β-HSD10 enzyme activity. **A)** Conversion of substrate (Acetoacetyl coenzymeA) to product uses NADH as a cofactor, converting it to NAD^+. The loss of absorbance of NADH at 340 nm (as it is converted to NAD^+) is directly proportional to the rate of 17β-HSD10 activity. When no 17β-HSD10 is present (black line) there is no NADH consumption in comparison to when 17β-HSD10 is present in the assay (red line). Background absorbance (buffer only) is shown also shown (blue line). **B)** Enzymatic activity obtained for 17β-HSD10 (μmol min^{-1} mg^{-1}) in the absence of amyloid at the different aggregation buffers used: (A) fibril-growing buffer: 10 mM Tris-HCl pH 7.5, 150 mM NaCl, 10 % (v/v) glycerol; (B) pH6 induced aggregation buffer: 50 mM MES pH 6.0; (C) HFIP-induced aggregation buffer: 50 mM Tris-HCl pH 7.9, 1.5% HFIP (v/v). **C)** Percentage of 17β-HSD10 enzyme activity remaining in the presence of 1 μM freshly prepared Aβ(1-42) under fibril (blue) and globule-growing (red) conditions at the indicated molar ratios of Aβ(1-42) and 17β-HSD10.

Figure 7. Comparative bar plots summarizing the relative variation in fluorescence self-quenching **A)** and ThT enhancement **B)** observed for the aggregation of 1 μM $A\beta_{555}$ and Aβ(1-42), respectively, into globules (red), fibrils (blue) and plaques (green) at Aβ: 17β-HSD10 molar ratios of 1:0 (control), 2:1

and 1:1. Data are expressed as the mean ± SEM from ≥ 3 separate experiments. ND indicates that no aggregation was detected.

Table of Contents

17β-HSD10 interaction with Aβ amyloid: what type of amyloid? 17β-hydroxysteroid dehydrogenase type 10 is a mitochondrial enzyme known to interact with β–amyloid (Aβ) aggregates and suppress Aβ-induced apoptosis in neurons, but the morphology of the amyloid aggregates predominantly inhibited by 17β-HSD10 remains unknown. A fluorescence self-quenching (FSQ) strategy was used to monitor the interaction in real time (left panel) and demonstrate that fibrils and globular aggregates, but not plaques, are specifically targeted by 17β-HSD10 (right panel).

10.1002/cbic.201600081

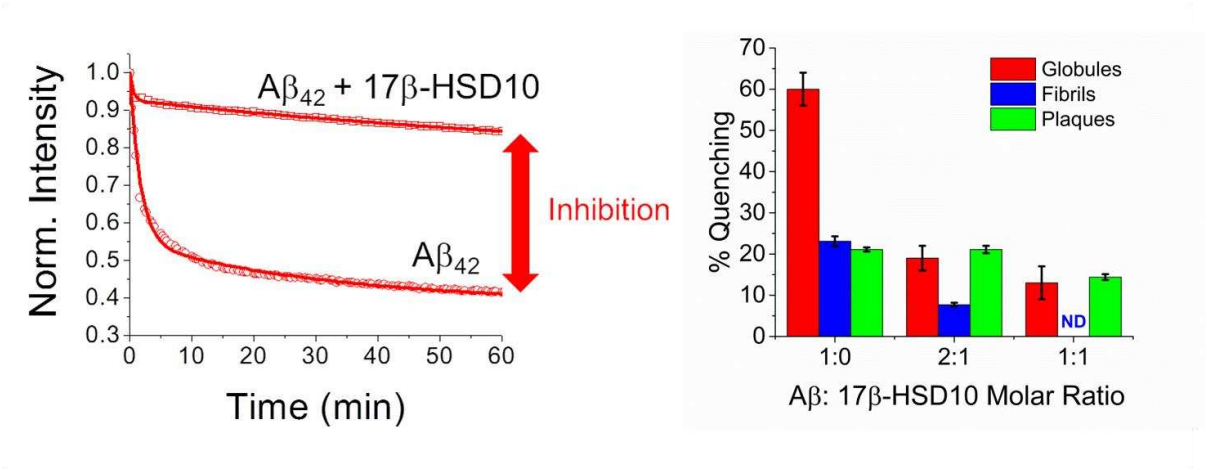

TOC

10.1002/cbic.201600081

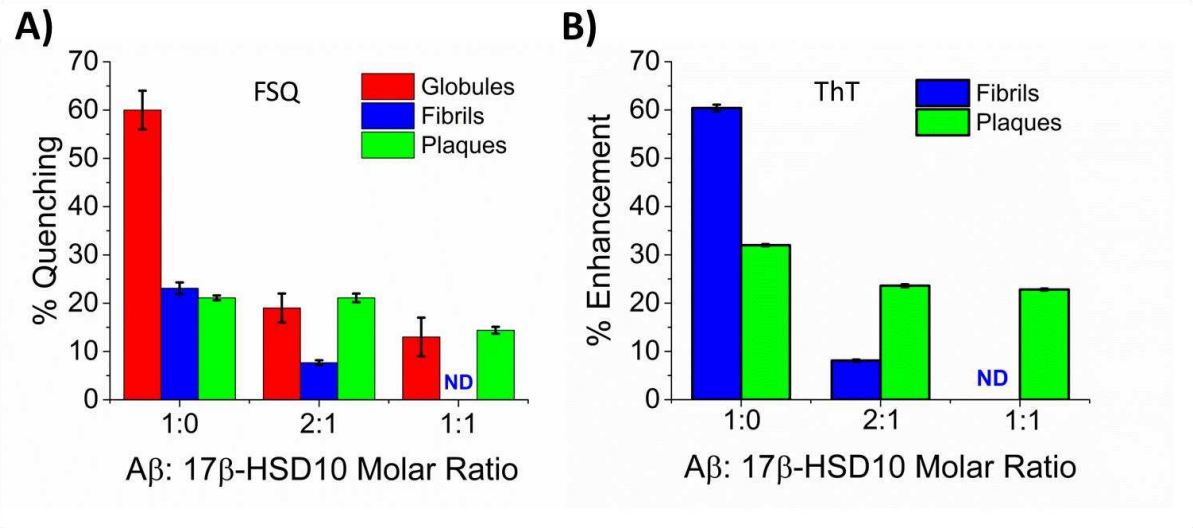

Figure 7

10.1002/cbic.201600081

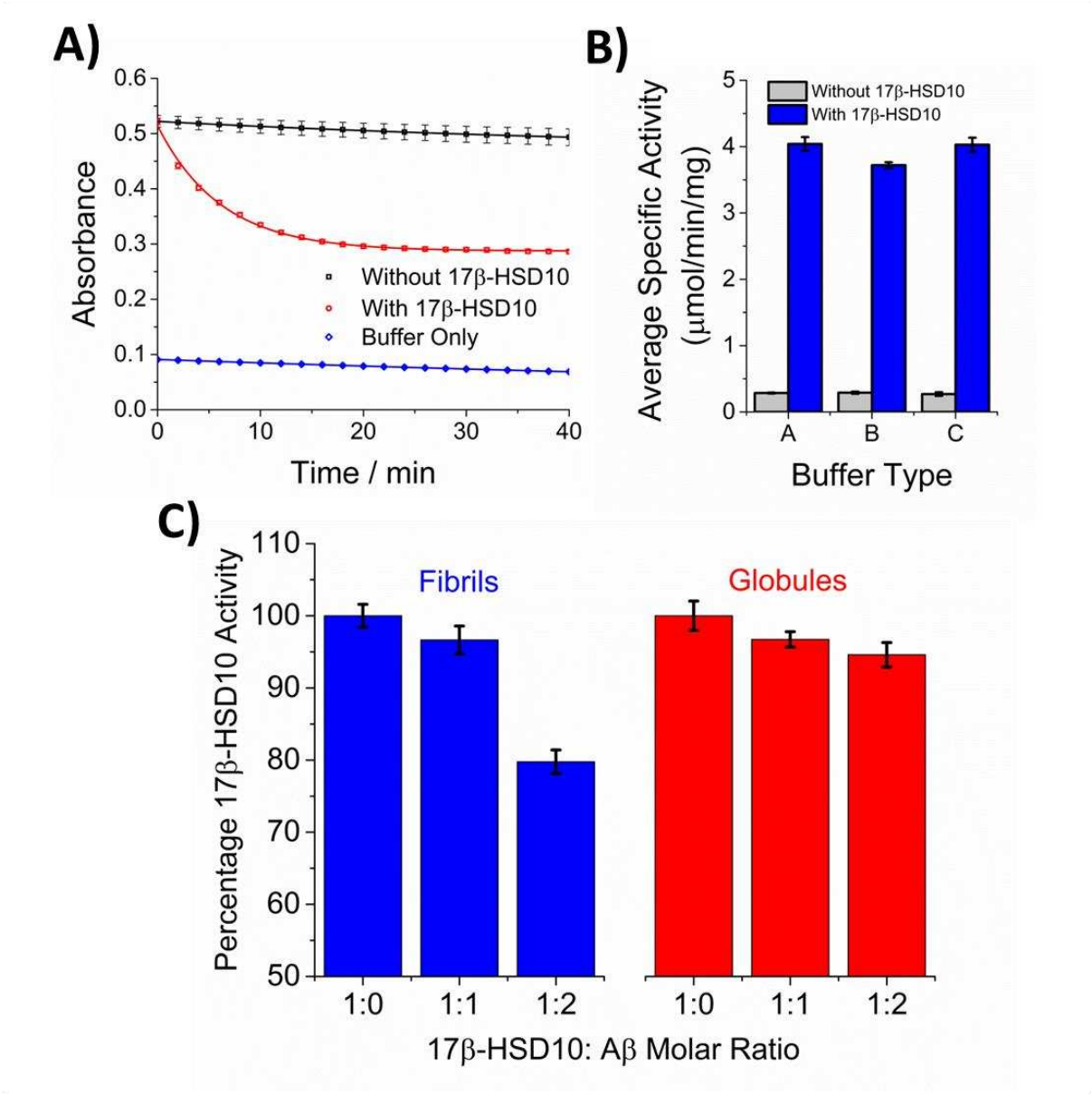

Figure 6

10.1002/cbic.201600081

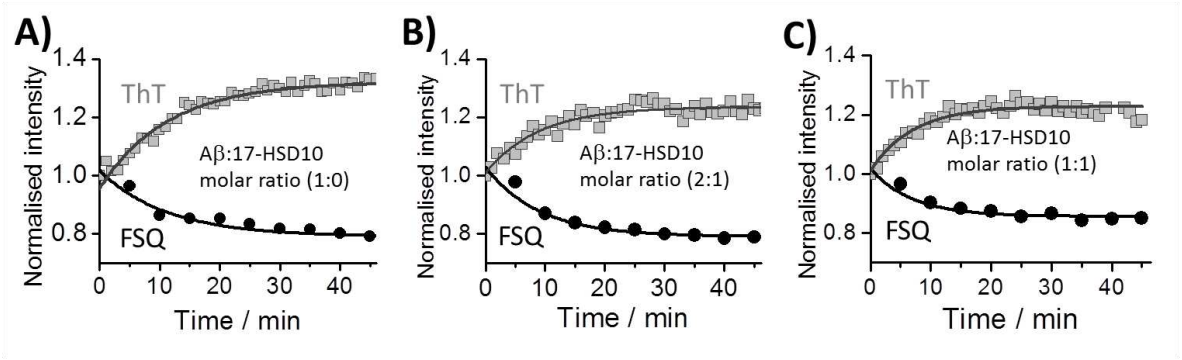

Figure 5

10.1002/cbic.201600081

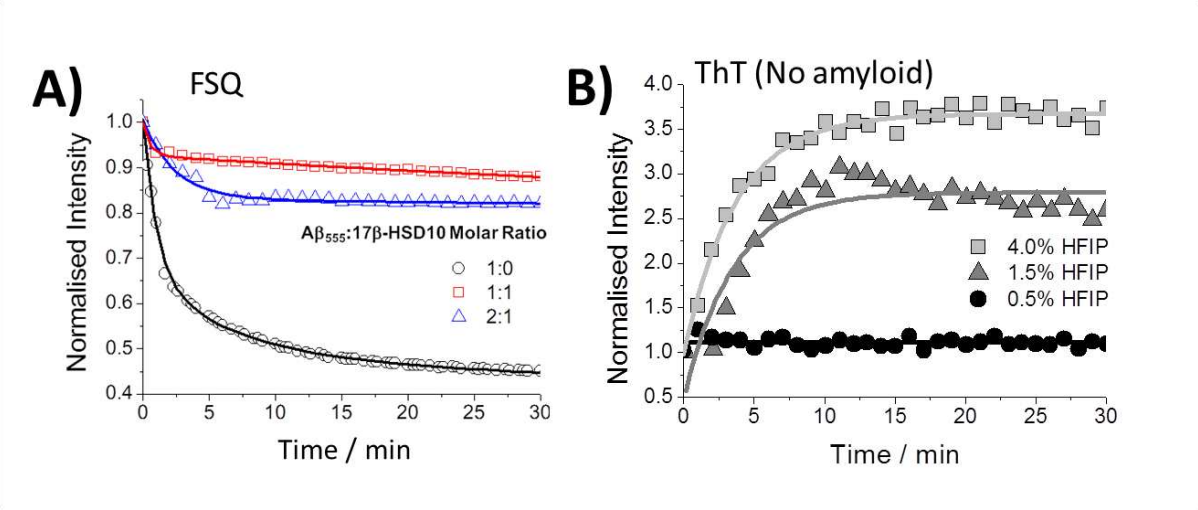

Figure 4

10.1002/cbic.201600081

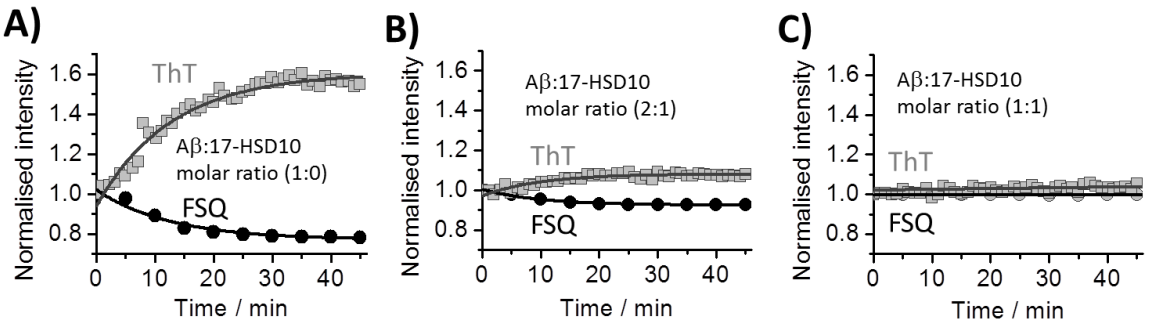

Figure 3

10.1002/cbic.201600081

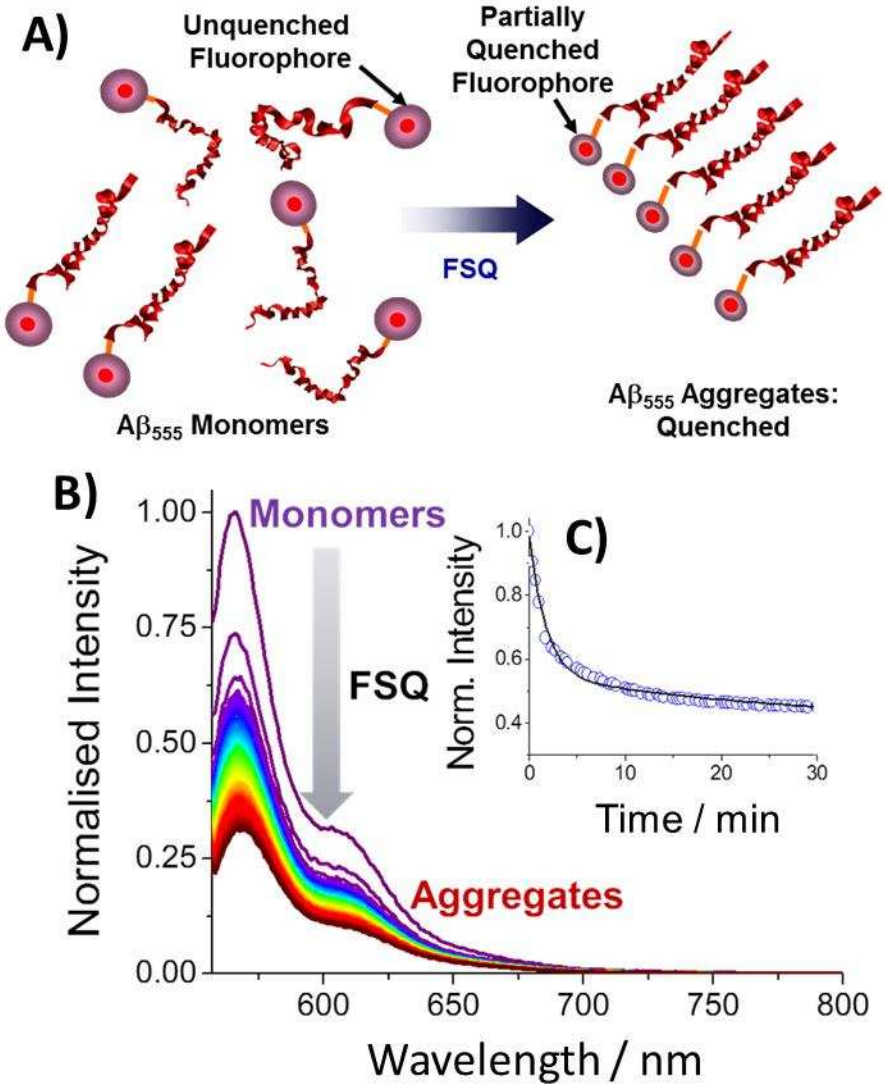

Figure 2

10.1002/cbic.201600081

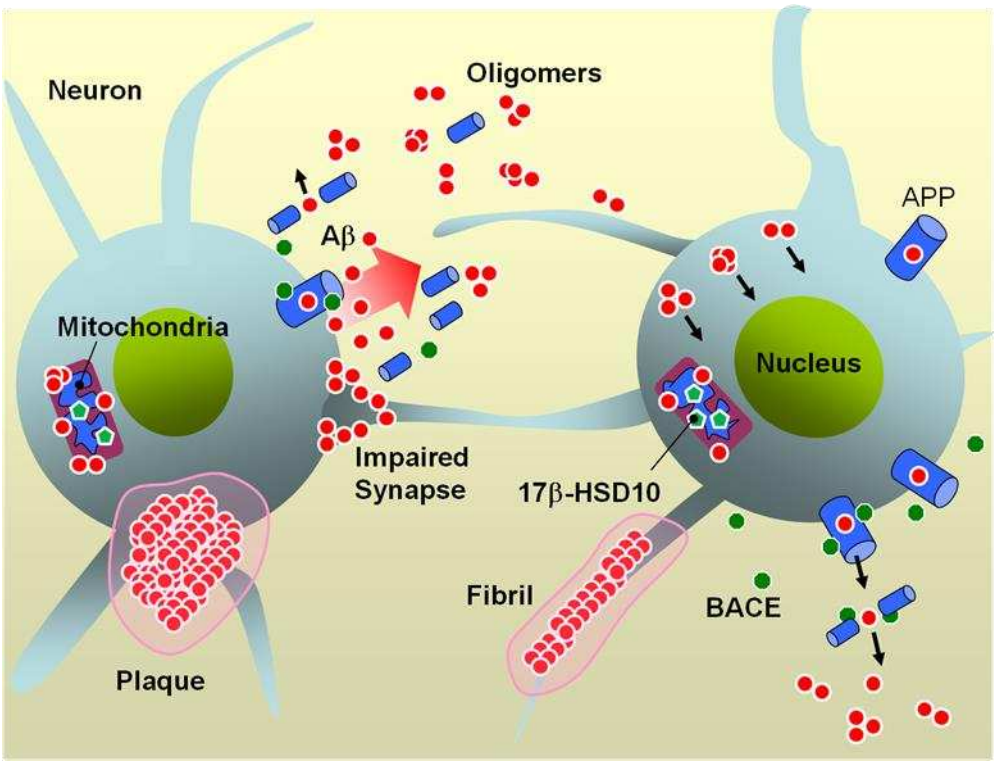

Figure 1